Optimization Of Ion Beam Elements Using Mathematical Transport Formalism

Mohamed Eisa[1*], J.L. Conradie[2], C. Mtshali[3], N. Mongwaketsi[3], and M. Maaza[3,4]

[1] Department of Physics, College of Science, Northern Border University, Arar, Saudi Arabia
[2] iThemba LABS-National Research Foundation, Accelerator Department, P.O. Box 722, Somerset West 7129, Cape Town, South Africa
[3] Materials Research Department, P.O. Box 722, Somerset West 7129, Cape Town, South Africa
[4] UNESCO-UNISA Africa Chair in Nanosciences & Nanotechnology Laboratories, College of Graduate Studies, University of South Africa, Muckleneuk Ridge, P.O. Box 392, Pretoria 0003, South Africa.
[*] Corresponding author. E-mail: memeisa@yahoo.com

Received: May 22, 2025; Accepted: Aug. 15, 2025

In the study we report the features and ideal stable operating conditions of the ion source and the accelerator's beam behavior of a nuclear microprobe at a laboratory for accelerator-based science (LABS) laboratory, i.e., iThemba LABS, South Africa. Since the aim is to improve the reliability and stability of ion beams used as a probe, we optimize the beam characteristics along the Van de Graaff accelerator from the ion source through the accelerator. Higher-order aberrations and non-ideal magnetic field profiles can induce complexities in beam deformation that are frequently missed by conventional first-order linear approximations. Moreover, the complicated nature and time commitment of trial-and-error methods make experimental adjustment alone inadequate. To accurately model and optimize the transport and focus characteristics of the ion beam, including effects from non-linear field components, dispersion, and alignment errors, a thorough mathematical framework is therefore required, backed by simulation tools such as TRANSPORT, TOSCA, and IGUN.

Keywords: beam line; emittance; beam intensity; ion source; microprobe; magnetic field

http://dx.doi.org/10.6180/jase.202607_30.027

1. Introduction

Although dipole magnets can also be made to help focus, quadrupole magnets are most frequently employed for beam focusing in beamlines between accelerators and between accelerators [1, 2] and external targets. Dipole magnets are utilized to change the direction of the beam. For many purposes, it is sufficient to calculate and present the behavior of particles with deviations in energy, position, and transverse momentum with respect to the central particle, through the beamline, in phase space, rather than calculating and studying the paths of numerous individual particles, representative of the beam, through the complex fields of beamline elements [3]. This has the advantage of avoiding a large number of trajectories and only requiring consideration of restricted regions in phase space [4, 5]. Due to Liouville's theorem, phase-space trajectories do not intersect, and initially bounded phase-space locations stay that way along the beamline. The behavior of the beam's boundary in phase space is consequently all that is required [6]. The six-dimensional phase space is typically used to characterize beam behavior in accelerators and beamlines [7]. The six dimensions are the longitudinal [1] position and energy deviations with regard to the center particle, the transverse (horizontal and vertical) [8] position deviations and divergence. Several papers have described the mathematical formulation of beam transport [9] elements and systems. The linear equations of motion and their applica-

tion to drift spaces and quadrupole and dipole magnets are first derived using the formulation of Carey [10, 11], and then the second order terms in the equations of motion are derived [12].

1.1. The linear equations of motion

The Lorentz force provides the time rate of change of momentum for a charged particle with velocity v and charge q in a static magnetic field B in the following vector differential equation of motion:

$$\dot{\mathbf{p}} = q(\mathbf{v} \times \mathbf{B}) \tag{1}$$

The magnitude of the momentum stays constant, and the Lorentz force is always perpendicular to the direction of motion. In order to remove time from Eq. (1), the center particle is now added; nevertheless, the new coordinates x, y, and t, respectively, define the position of an arbitrary particle with respect to the central particle in the horizontal, vertical, and longitudinal directions. The equation of motion is as follows in the new coordinate system [13]:

$$\frac{d^2\mathbf{T}}{dT^2} = \frac{q}{p}\frac{d\mathbf{T}}{dT} \times \mathbf{B} \tag{2}$$

Where the location and travel length of an arbitrary particle are denoted by the vector T and the scalar t, respectively. The particle's trajectory's unit vector tangent is $\frac{d\mathbf{\Gamma}}{dT}$. The three mutually perpendicular unit vectors $\mathbf{x}, \mathbf{y}, \hat{\mathbf{t}}$ along the three coordinate axes satisfy the following relations:

$$\begin{aligned} \hat{\mathbf{x}} &= \hat{\mathbf{y}} \times \hat{\mathbf{t}} \\ \hat{\mathbf{y}} &= \mathbf{t} \times \hat{\mathbf{x}} \\ \mathbf{t} &= \hat{\mathbf{x}} \times \hat{\mathbf{y}} \end{aligned} \tag{3}$$

The derivatives of the unit vectors with respect to t are given by:

$$\begin{aligned} \hat{\mathrm{x}}' &= h\hat{\mathrm{t}} \\ \hat{\mathrm{y}}' &= 0 \\ \hat{\mathrm{t}}' &= -h\hat{\mathrm{x}} \end{aligned} \tag{4}$$

where the rate of direction change in relation to path length is the definition of h, the curvature of a trajectory. Additionally, the reciprocal of the central trajectory's local radius of curvature (ρ_0) is the curvature $h(t)$ [14]. For the azimuthal distance in cylindrical coordinates, the term $\rho \mathrm{d}\theta$ is expressed as $(1 + \mathrm{hx})$, where $(1 + \mathrm{hx})$ denotes the relative sizes of ρ and $\rho 0$. The differential line element along any given trajectory can be found using [15]:

$$d\mathbf{T} = \mathbf{x}dx + \mathbf{y}dy + (1 + hx)\hat{\mathbf{t}}dt \tag{5}$$

The two transverse components of the equation of motion now become:

$$\begin{aligned} x'' - h(1 + hx) &= \frac{q}{p}(1 + hx)[y'B_t - (1 + hx)B_y] \\ y'' &= \frac{q}{p}(1 + hx)[1 + hx)B_x - x'B_t] \end{aligned} \tag{6}$$

For the central particle x and y as well as their derivatives are equal to zero and the following equation is obtained:

$$h = \frac{q}{p_0}B_y(0, 0, t) \quad \text{or} \quad B\rho_0 = \frac{p_0}{q} \tag{7}$$

In any region of space containing no electric currents, the field of a static electromagnet can be expressed in terms of a scalar potential Φ so that:

$$\mathbf{B} = \nabla\Phi \tag{8}$$

Here, the typical negative sign is regarded as part of the potential. The field component, the y -direction, which is generated by differentiating the potential with respect to y, can only include constant and even powers in y due to the mid-plane symmetry [16]. Therefore, only unequal powers should be present in an expansion of the scalar potential in a power series, y. Additionally, only linear terms in x and y contribute to the first-order equations of motion. As a result, only quadratic terms in the equations above [17] are taken into consideration.

$$\mathrm{F}(x, y, t) = A_{10}y + A_{11}xy \tag{9}$$

where t determines the values of the coefficients. Only in second and higher orders does Laplace's equation impose relationships between the coefficients, thus the two can be selected independently. Then, [18] provides the magnetic field's constituent parts:

$$\begin{aligned} B_x(x, y, t) &= \frac{\partial\Phi}{\partial x} = A_{11}y \\ B_y(x, y, t) &= \frac{\partial\Phi}{\partial y} = A_{10} + A_{11}x \\ B_t(x, y, t) &= \frac{1}{(1 + hx)}\frac{\partial\Phi}{\partial t} = A'_{10}y + \left(A'_{11} - hA'_{10}\right)xy \end{aligned} \tag{10}$$

The coefficient A_{11} can be expressed in terms of a dimensionless parameter n so that:

$$\begin{aligned} A_{10} &= \frac{hp_o}{q} \\ A_{11} &= -hA_{10}n \end{aligned} \tag{11}$$

The field index n is given in terms of the vertical magnetic field component by:

$$n = \left[\frac{1}{hB_y}\left(\frac{\partial B_y}{\partial x}\right)\right]_{\substack{x=0\\y=0}} \tag{12}$$

The expressions for the components of the magnetic field from Eqs. (10) and (11) can now be substituted into the equations of motion. A new quantity $\delta = \frac{\Delta p}{p_0}$, the fractional deviation of the momentum from that of the central trajectory, is defined by:

$$p = p_0(1+\delta) \tag{13}$$

By making use of the equation of motion for the central trajectory and by retaining only terms of first order the following equations are obtained from Eq. (6).

$$\begin{aligned} x'' + (1-n)h^2 x &= h\delta \\ y'' + nh^2 y &= 0 \end{aligned} \tag{14}$$

The general solution of the differential equations 14 for x and y as functions of t can be written in terms of sine-like functions, $s_x(t)$ and $s_y(t)$, cosine-like functions, $c_x(t)$ and $c_y(t)$ and their derivatives as well as a dispersion function $d_x(t)$:

$$\begin{aligned} x(t) &= x_0 c_x(t) + x_0' s_x(t) + \delta d_x(t) \\ y(t) &= y_0 c_y(t) + y_0' s_y(t) \end{aligned} \tag{15}$$

where x_0, x_0', y_0, y_0' are the respective initial values. The sine- and cosine-like functions are solutions of the homogeneous equations. The function $d_x(t)$ is a particular integral of the first of equations 14 and can be obtained by means of Green's function G [19]:

$$G(t,t) = s(t)c(\tau) - c(t)s(\tau) \tag{16}$$

$$d_x(t) = s_x(t)\int_0^t c_x(\tau)h(\tau)d\tau - c_x(t)\int_0^t s_x(\tau)h(\tau)dt \tag{17}$$

Using equations 14 the solutions for x, x', y, and y' can be expressed in terms of the following matrix equations:

$$\begin{aligned} \begin{pmatrix} x(t) \\ x'(t) \\ \delta \end{pmatrix} &= \begin{pmatrix} cx(t) & s_x(t) & d_x(t) \\ c_x'(t) & s_x'(t) & d_x'(t) \\ 0 & 0 & 1 \end{pmatrix} \begin{pmatrix} x_0 \\ x_0' \\ \delta \end{pmatrix} \\ \begin{pmatrix} y(t) \\ y'(t) \end{pmatrix} &= \begin{pmatrix} c_y(t) & sy(t) \\ c_y'(t) & s_y'(t) \end{pmatrix} \begin{pmatrix} y_0 \\ y_0' \end{pmatrix} \end{aligned} \tag{18}$$

The total transfer matrix R_t for a beamline is obtained by multiplication of the matrices $R_1, R_2, \ldots R_n$ for the individual segments of the beamline:

$$R(T) = R_n \ldots R_2 R_1 \tag{19}$$

The full six by six transfer matrix for linearized motion in a static magnetic system with mid-plane symmetry now becomes [20, 21]:

$$\begin{pmatrix} x(t) \\ x'(t) \\ y(t) \\ y'(t) \\ \ell(t) \\ \delta(t) \end{pmatrix} = \begin{pmatrix} R_{11} & R_{12} & 0 & 0 & 0 & R_{16} \\ R_{21} & R_{22} & 0 & 0 & 0 & R_{26} \\ 0 & 0 & R_{33} & R_{34} & 0 & 0 \\ 0 & 0 & R_{43} & R_{44} & 0 & 0 \\ R_{51} & R_{52} & 0 & 0 & 1 & R_{56} \\ 0 & 0 & 0 & 0 & 0 & 1 \end{pmatrix} \begin{pmatrix} x_0 \\ x_0' \\ y_0 \\ y_0' \\ \ell_0 \\ \delta_0 \end{pmatrix} \tag{20}$$

Since particles in the median plane experience no force in the vertical direction the matrix elements $R_{31}, R_{32}, R_{35}, R_{36}, R_{41}, R_{42}, R_{45}, R_{46}$ are zero. Because only static magnetic fields and no electric fields are considered the particle energy remains constant [22]. $R_{61}, R_{62}, R_{63}, R_{64}, R_{65}$ are therefore zero and R_{66} is equal to one. With the exception of bunches, which are not taken into account here, forces acting on particles are independent of their longitudinal location, so $R_{15}, R_{25}, R_{35}, R_{45}$, and R_{65} are all zero. The vertical beam displacement's contribution to the longitudinal position is disregarded in the linear approximation of the equations of motion. Thus, R_{53} and R_{54} are both zero [14, 23]. The results show that $R_{36}, R_{46}, R_{13}, R_{14}, R_{23}$, and R_{24} are zero in the same approximation because the momentum spread does not contribute to the vertical motion and the vertical motion does not contribute to the horizontal motion. The path length difference expressed in terms of the initial coordinates is given by:

$$\ell = x_0\int_0^t c_x(\tau)h(\tau)d\tau + x_0'\int_0^t s_x(\tau)h(\tau)d\tau + \delta_0\int_0^t d_x(\tau)h(\tau)d\tau \tag{21}$$

The matrix elements related to path length in the six-by-six matrices can be evaluated from:

$$\begin{aligned} R_{51} &= (\ell \mid x_0) = \int_0^t c_x(\tau)h(\tau)d\tau \\ R_{52} &= (\ell \mid x_0') = \int_0^t s_x(\tau)h(\tau)d\tau \\ R_{56} &= (\ell \mid \delta) = \int_0^t d_x(\tau)h(\tau)d\tau \end{aligned} \tag{22}$$

The longitudinal separation, or the distance that the central particle is behind a particle with momentum p traveling a route length L , at the end of the beamline is determined by the following formula for a length L_0 of the reference trajectory and the velocity v_0 of the central particle:

$$\ell = L - L_0 - L_0\frac{1}{\gamma^2}\delta \tag{23}$$

Where $\gamma^2 = 1 - \frac{v^2}{c^2}$ and c the velocity of light in vacuum.

1.2. The transfer matrices of some beamline elements

Transfer matrices of a drift space. A drift space, a field-free area in the beamline that is defined by a single parameter L , the length, is the most basic beamline element. Both n and h are 0 in such a region, and the longitudinal and transverse momenta are conserved. Equations 14 and this indicate that [4, 5]:

$$\begin{aligned} &x'' = 0,\ y'' = 0,\ x'(t) = x_0',\ y' = y_0', c_x(t) = 1,\ c_y(t) = 1,\\ &s_x(t) = t,\ s_y(t) = t,\ d_x(t) = 0 \end{aligned} \tag{24}$$

and at the end of the drift space:

$$\begin{aligned} &x(\ L) = x_0 + x_0' L, y(\ L) = y_0 + y_0' L\\ &x'(L) = x_0', y'(L) = y_0' \end{aligned} \tag{25}$$

Since h is equal to zero the only contribution to the change in path length due to the momentum spread is:

$$\ell = -L\frac{1}{\gamma^2}\delta$$

To follow the convention commonly used in the literature on beam transport [19] theory the minus sign is left out in the following matrix R for a drift space [19, 20], to indicate the distance that the particle with momentum p is ahead of the central particle at the end of the drift space [16, 19]:

$$R = \begin{pmatrix} x(t)\\ x'(t)\\ y(t)\\ y'(t)\\ \ell(t)\\ \delta(t) \end{pmatrix} = \begin{pmatrix} 1 & L & 0 & 0 & 0 & 0\\ 0 & 1 & 0 & 0 & 0 & 0\\ 0 & 0 & 1 & L & 0 & 0\\ 0 & 0 & 0 & 1 & 0 & 0\\ 0 & 0 & 0 & 0 & 1 & L/\gamma^2\\ 0 & 0 & 0 & 0 & 0 & 1 \end{pmatrix} \begin{pmatrix} x_0\\ x_0'\\ y_0\\ y_0'\\ \ell_0\\ \delta_0 \end{pmatrix} \tag{26}$$

1.3. Transfer matrices for a quadruple magnet

In quadrupole and dipole magnets the magnetic field is in most cases constant along the path of the central trajectory. In such cases the homogeneous form of Eq. (14) can be written as [19, 20]:

$$q'' \pm k^2 q = 0 \tag{27}$$

For the positive sign the functions $c(t)$ and $s(t)$ are now:

$$\begin{aligned} c(t) &= \cos kt\\ s(t) &= \frac{1}{k}\sin kt \end{aligned} \tag{28}$$

For the negative sign in Eq. (27) the trajectory is divergent [24] and the general solution can be expressed as:

$$\begin{aligned} c(t) &= \cosh kt\\ s(t) &= \frac{1}{k}\sinh kt \end{aligned} \tag{29}$$

The dispersion function is given by:

$$d_x(t) = \frac{h}{k_x^2}\left(1 - c_x(t)\right) \tag{30}$$

The scalar potential of the field of a quadrupole magnet can be obtained by conformal mapping and is in rectangular coordinates given by [11, 20]:

$$\Phi = \frac{B_0 xy}{a} \tag{31}$$

where B_0 is the magnetic field on a pole tip at a point closest to the optical axis $x = 0, y = 0$ and a is the distance from the origin to this point. The magnetic field components can be expressed as the gradient of the scalar potential [5]:

$$\begin{aligned} B_x &= \frac{B_o y}{a} = gy\\ B_y &= \frac{B_0 x}{a} = gx \end{aligned} \tag{32}$$

The magnitude of the field B as a function of the radius r is given by:

$$B = gr \tag{33}$$

The field has the following symmetry about both horizontal and vertical planes:

$$\begin{aligned} B_x(x,y,t) &= -B_x(x,-y,t) = B_x(-x,y,t)\\ B_y(x,y,t) &= B_y(x,-y,t) = -B_y(-x,y,t) \end{aligned} \tag{34}$$

In a quadrupole magnet the curvature h of the central trajectory is zero and Eq. (36) become:

$$\begin{aligned} x'' &= -\frac{q}{p}B_y\\ y'' &= \frac{q}{p}B_x \end{aligned} \tag{35}$$

With the field components substituted from Eq. (35) the following equations of motion for a quadrupole magnet are obtained:

$$\begin{aligned} x'' + k_q^2 x &= 0\\ y'' - k_q^2 y &= 0 \end{aligned} \tag{36}$$

with:

$$k_q^2 = \frac{qg}{p_0} \tag{37}$$

Eqs. (32), (36) and (37) show that for positive field strength the beam is focused horizontally and defocused vertically [20]. The solutions to these Eq. (36) are given by Eqs. (28) and (29) for the x - and y -directions, respectively. Since the central trajectory has no curvature the change in

path lengths due to the momentum spread is again given by the same expression $L\frac{1}{\gamma^2}\delta$ as for a drift space, with L the length of the magnet. For the same reason the dispersion function d_x is also zero. The transfer matrix R for a quadrupole magnet [25].

2. The computer programs

2.1. Transport [10]

Input file for the TRANSPORT program from ion source to the end of the accelerator tube (algorithm 1).

2.2. IGUN

This program (algorithm 2) has built in boundary processing of PLYGON, which gives a CAD-like user interface to set up the boundary, including definition of internal electrodes, dielectric boundaries, and slanted Neumann boundaries (field lines as boundary elements). The input now is mesh independent and can use any coordinates from a drawing, accepting any offset. The output of the equipotentials, field line and trajectories (to be used in a further run) has the same offset and units, which greatly eases the organization of concatenated runs Ext_106c.in (90/65mA, Positive EE, EE by Dan).

2.3. TOSCA

The TOSCA program is not a traditional standalone "computer program" you script directly like Python or Fortran. Rather, TOSCA is a graphical simulation software integrated into the Opera Simulation Suite (by Vector Fields, now owned by Dassault Systèmes), and it's used mainly for 3D magnetostatic field analysis — particularly in electromagnet design, such as ion sources, quadrupoles, and beamline magnets. However, you can interface with TOSCA computationally through input files, macro scripts, and batch commands. Here's how TOSCA works in a programmable or computational context (algorithm 3).

3. Results and discussions

TOSCA main role is 3D field computation (detailed B-fields from magnet design) the sections on static magnetic fieldsm, that is related to scalar/vector potentials. IGUN main role is Ion beam extraction and early beam dynamics that is related to the sections on Lorentz force, initial equations of motion.

TRANSPORT main role is Beam transport optics through magnets and drift spaces (matrix formalism) and that is related to the sections on transfer matrices, drift/quadrupole magnets, dispersion, Table 1 presents the program and it is relation with the mathematical formalism.

Algorithm 1

```
/Ion Source+Lens+Accelerator tube. /
0  (Indicator card means the following describes a new problem
15. 11.0 /MEV/ 0.001; (Input-output units)
15. 1.0 /MM/ 0.1;
1. 17170.0.4.3323/BEAM/;    (Guess of initial beam parameters)
16. 4.0 100.0;    (Special input parameters)
16. 31837.7 /MASS/    (Mass of the particles comprising the beam,
in units of electron mass)
3. .061 /D/;   (Drift Space)
6. 1.043 .04;   (Transformation matrix update)
3. .02/D/;
11. 0.0 .0029;
11. 0.0021;   (Electrostatic acceleration section)
11. .02 1;
11. 0.002 0.0;
3. .019/D/;
6. 1.043 .04;
3. .081;
6. 1131;
3. .002/D/;
3. .075/D/;
11. 0.0 .0028;
11. 0.0051 ;
11. .05 1;
11. .014 0.0;
   3. .461/D/;
6. 1 15 3 15;
11. 0.0 0.0064,
11. .01 1;
11. .09 1;
11. .01 0;
3. .118/D/;
6. 1 15 3 15;
3. .012/D/;
11. .0 5.988;
11. .027 .0051;
11. .027 .0103 ;
11. .027 .0153;
11. .027 .0205;
11. .027 .0256;
11. .027 .0307;
3. 1.0 /D/ ;
13. 48 ;   (Bending magnet input specification)
16. 7.0 .7 ;
16. 7.0 .45;
16. 8.0 2.8;
13. 1.0;
13. 3.0;
3. .109 /L1/;
5.01 .110 -1.5 22.5/QUAD1/;    (First electrostatic quadrupole lens)
3. .085 /L2/;
13. 1.0;
5.01 .110 1.5 22.5 /QUAD2/;    (Second electrostatic quadrupole lens)
3. .440 /L3/;
10. 1.0 1.0 .5 0.1 /FIT1/;    (Fitting beam size to y_max=0.5 mm)
10. 3.0 3.0 .5 0.1 /FIT2/;    (Fitting beam size to y_max=0.5 mm)
SENTINEL (Plotting the TRANSPORT run to view the fitted bean envelope)
/*PLOT*/
SENTINEL    (First one signifies the problem is terminated)
SENTINEL    (The second one signifies the end of the TRANSPORT run)
```

Table 1. outlines the fundamental mathematical concepts underlying charged particle beam simulation and design. It highlights how each formalism ranging from Lorentz force dynamics to matrix-based transport methods is implemented or utilized within the TOSCA, IGUN, and TRANSPORT software tools, emphasizing their complementary roles in modeling magnetic fields, beam optics, and particle trajectories.

Mathematical formalism	It is relation with TOSCA, IGUN, and TRANSPORT
Lorentz Force, Equation of Motion	All three programs rely on solving the Lorentz force equation, either exactly (simulation) or approximately (matrix methods).
Coordinate System (x, y, t)	IGUN and TRANSPORT especially use this formalism: small displacements around a "central trajectory."
Curvature h(t), Radius of Curvature ρ_0	Important for TRANSPORT - it uses curvature to define bending magnets and how particles deviate from the reference path.
Static Magnetic Fields (Scalar Potential ϕ)	TOSCA computes detailed 3D magnetic field maps (using finite elements), based on Maxwell's equations (including scalar/vector potentials).
Field Expansions (Taylor Series)	TRANSPORT uses Taylor series expansions of magnetic fields to calculate beam behavior through magnetic elements (dipoles, quadrupoles, etc.).
First-order Equations of Motion	TRANSPORT uses the linearized version to construct transfer matrices for different beamline elements.
Matrix Formalism (Transfer Matrices)	TRANSPORT is completely based on this. It calculates how particle beams evolve through a series of magnets using 6x6 transfer matrices.
Dispersion Function	TRANSPORT calculates dispersion (how particles with slightly different momentum spread out spatially), important for designing beamlines.
Drift Spaces, Quadrupoles	IGUN can simulate simple spaces and electrodes, while TRANSPORT models these beamline elements using their matrices.
Focusing/Defocusing (Quadrupoles)	IGUN simulates initial extraction and focusing, TRANSPORT handles subsequent beamline focusing using matrix methods.

The TRANSPORT software, which is frequently used to compute ion beam transport, mainly uses matrix techniques to represent and work with the ion beam's phase space. An ion beam is more than just a group of particles at one location, according to phase space representation. It has a distribution in momentum (or angle) as well as location. Phase space is a six-dimensional space that has three position coordinates and three momentum/angle coordinates. This is simplified by TRANSPORT, which frequently takes into account 2D slices of phase space (such as the x and x' angle). One way to depict the particle distribution in this 2D space is via a matrix. The envelope (the boundary with the majority of particles) of the beam is commonly described using a second-order matrix (R-matrix).

Matrix transformations include the phase space distribution of the beam is impacted by optical components in the beamline, such as quadrupoles, drift spaces, and bending magnets. Mathematical matrices can be used to depict these transformations. The impact of these components on the beam is simulated by TRANSPORT using matrix multiplication. The original beam-representing phase space matrix is multiplied by a sequence of optical element-representing matrices. Following its passage through the element, the beam's phase space is described by a new matrix. In order to determine the beam's characteristics (size, divergence, and shape) at any given location, TRANSPORT [25, 26] repeats this procedure for every element in the beamline.

With the σ-matrix formalism, the behavior of a beam of particles in a beamline can be computed and displayed in phase space using the transfer matrices for the linearized motion of individual particles, which can be expanded to include the vertical and longitudinal motion. The computer software TRANSPORT [9] uses the linearized or first order equations mentioned above for the fundamental beamline design. The second-order differential equations of motion individual particle trajectories can be computed by numerically solving the full equations of motion using interpolated field values from predicted or recorded magnetic field maps in order to assess second and higher order effects in a beamline. The computer software TOSCA, which will be covered shortly, employs this technique. The data can also be shown in phase space by choosing several particles that are indicative of the entire beam. Another approach is to add second order matrix elements to the matrix method previously employed.

The software programs TRANSPORT models the mo-

Algorithm 2

```
&INPUT1 RLIM=45,ZLIM=5285,POTN=4,
POT=0,4705,0,-8326, &END
3, 0, 0 (electrode No 3, and R, Z are polar coordinates)
3, 44, 0
2, 44, 5
2, 1, 5
2, 2.5, 7
2, 3.5, 9
2, 7.83309, 9
1002, 7.833095, 10.8
-1.8
2, 8.16406, 9.03069
2, 25, 22
2, 44, 22
1, 44, 34
1, 30, 34
1, 8, 13
1, 4, 76
1, 8, 95
1, 11, 95
4, 9.300003, 97
4, 9.300003, 118
4, 26, 1184, 31, 119
1, 38, 124
1, 38, 140
1, 12.3, 140
1, 12.3, 121
1, 9.300003, 121
1, 9.300003, 140
1, 4, 140
1, 4, 142
1, 44, 224
1, 0, 224
3, 0, 0
&INPUT5 MAXRAY=30, STEP=0.05, TE=4, UI=0, MASS=1,
RP=2, ZP=1, NS=15, HOLD=15, PDENS=5.7E11,
AMPSO=0.00050,NSCAN=2,SY=8,DSCAN=5,ZSCAN=0,
LASER=T,WRTEQU=-5000 &END
   &BUNDLE RB2=4 &END
```

Algorithm 3

```
! Define model
BEGIN MODEL
   NAME = 'solenoid'
   UNITS = 'mm'
END
! Define material
DEFINE MATERIAL
   NAME = 'Copper'
   TYPE = 'Conductor'
END
! Define geometry
BLOCK
   NAME = 'Coil'
   SIZE = (50, 100, 50)
   POSITION = (0, 0, 0)
   MATERIAL = 'Copper'
END
! Apply excitation
CURRENT = 1000    ! Amps
! Set boundary
AIRBOX
   SIZE = (500, 500, 500)
   TYPE = 'open'
END
! Mesh
MESH DENSITY = 'fine'
! Run solver
SOLVE
! Export B-field map
EXPORT FIELD = 'coil_field.tab'
```

tion of beams of charged particles (such as ions, electrons, etc.) via drift spaces and a sequence of magnetic elements (such as quadrupoles, sextupoles, and dipoles). At different places along the beamline, its main objective is to forecast and regulate the beam's characteristics (size, shape, and divergence) [8, 9]. IGUN is a popular computer program made especially for simulating and designing charged particle beam transport systems, including injectors and ion guns. IGUN's purpose is to use electromagnetic fields to imitate the paths of charged particles, such as electrons or ions. This enables users to design beam transport lines, accelerating structures, and ion sources as efficiently as possible. However, Specifically, TRANSPORT is used to calculate the beam envelope based on the experimentally applied voltages across different lens elements, as depicted in Fig. 1. This helps visualize and assess how well the beam is guided and focused through the system [21, 23] On the other hand, Fig. 2 presents the results from a simulation using IGUN, which models the beam extraction and initial acceleration at the high-voltage terminal of the Van de Graaff accelerator. IGUN focuses particularly on ion optics and beam formation near the ion source, providing crucial initial conditions for downstream beam transport simulations. Both the voltages on the electrodes and the current at the second collimator downstream from Einzel lens 2 were provided. Fig. 3 shows the beam envelopes computed using the computer program TOSCA. The beam profile was determined using the voltages on the electrodes, which were obtained by optimizing the beam through the Van de Graaff accelerator. Several particle trajectories with varying angular deviations and the same initial position are displayed. The voltages on the electrodes are the same as those which have been used with the program IGUN in Fig. 2. This presented the detailed investigation of the beam optics as well as the modifications to improve the transmission through the accelerator and the beam intensity.

4. Conclusion

In order to calculate the accelerator's beam optical properties, measurements and documentation of the electrodes' sizes and separations were made. These calculations have been performed using various computer programs, starting from the ion source and continuing through the terminal section, accelerator, beam line up, and Nuclear Microprobe (NMP). For the beam optics in the terminal portion, the results from the computer programs TOSCA and IGUN, which account for space-charge effects, were comparable to the experimentally found optimum voltages on the various lenses. However, because the computer program TRANS-

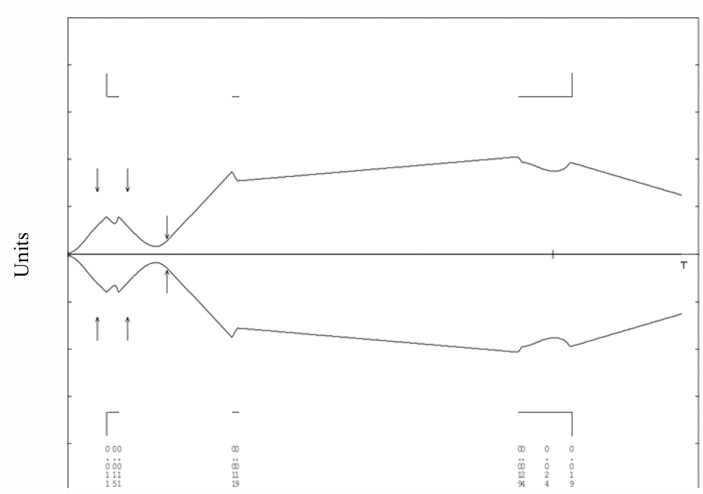

Fig. 1. Beam envelope calculated with the program TRANSPOR. The trajectories of two particles with the same starting position but different angular deviations are shown. The voltages on the electrodes are the same as that which have been used with the program IGUN and TOSCA.

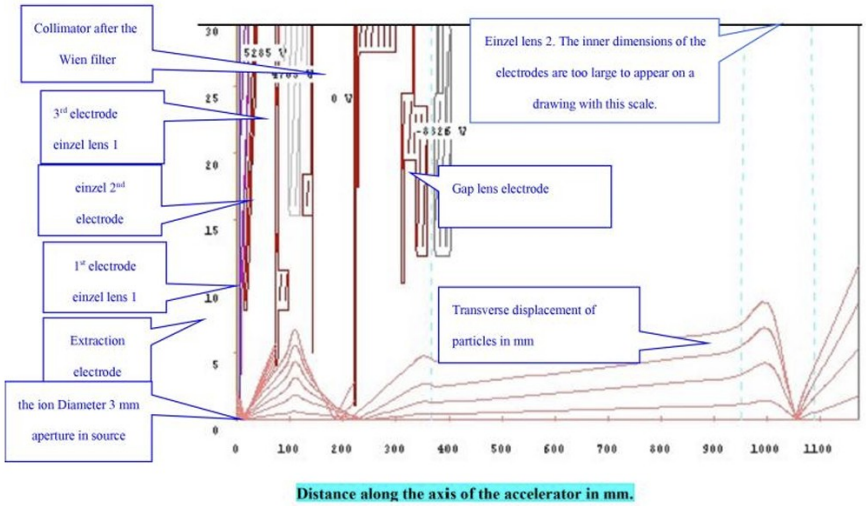

Fig. 2. Transverse beam dimensions in mm, in the high-voltage terminal section of the Van de Graaff accelerator, calculated with the program IGUN for a round ion source aperture of 3 mm diameter. The potential differences between the electrodes in the figure are the same as in the accelerator, but the absolute values differ. The ion source, as well as the collimator after the Wien filter, is at zero potential. The potential of the extraction electrode is 5285 Volt. The second electrode of the first einzel lens is at 4705 Volt. The electrode of the gap lens is at a potential of –8325 Volt. The beam envelope up to and through the second einzel lens is shown. The collimators intercept some of the particles.

PORT does not account for various lens forms, it is not appropriate for precisely calculating beam profiles through intricate electrostatic lenses. The voltage and the distances between a lens's several portions are the only parameters that can be set in TRANSPORT. However, the gap sizes of the various lenses can be adjusted to produce the same beam envelope with TRANSPORT as achieved with TOSCA and IGUN if the beam envelope is known from calculations made using those programs. With these adjusted gap sizes, TRANSPORT, which is simpler and quicker to use, can be used to perform additional computations for various energies and lens settings.

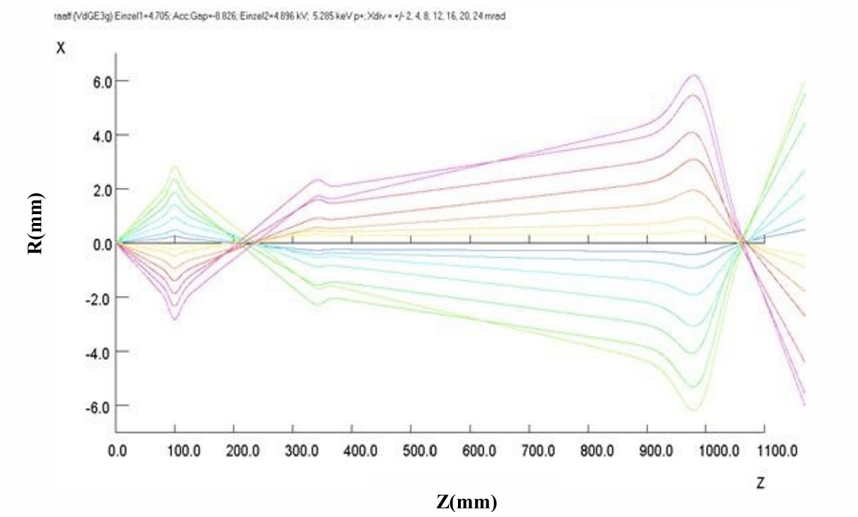

Fig. 3. TBeam envelopes calculated with the computer program TOSCA. The trajectories of a number of particles with the same starting position but different angular deviations are shown. The voltages on the electrodes are the same as those which have been used with the program IGUN in Fig. 2 above.

Acknowledgements

The authors thank the Deanship of Scientific Research at Northern Border University, Arar, Kingdom of Saudi Arabia for funding this research work through project number NBU-FFR-2025-0052-03.

References

[1] M. Szilagyi, (1981) *"A novel Approach to Beam Optics Design for Particle Accelerators"* **Particle Accelerators *1***: 213–217.

[2] S. Marini, D. F. G. Minenna, F. Massimo, L. Batista, V. Bencini, A. Chancé, N. Chauvin, S. Doebert, J. Farmer, E. Gschwendtner, L. Moulanier, P. Muggli, D. Uriot, B. Cros, and P. Nghiem, (2024) *"Beam physics studies for a high charge and high beam quality laser-plasma accelerator"* **Physical Review Accelerators and Beams *27***(063401): 1–15. DOI: 10.1103/PhysRevAccelBeams.27.063401.

[3] B. Hermann et al., (2021) *"Electron beam transverse phase space tomography using nanofabricated wire scanners with submicrometer resolution"* **Physical Review Accelerators and Beams *24***(2): 022802. DOI: 10.1103/PhysRevAccelBeams.24.022802.

[4] A. E. Stuchbery, (1996) *"Beam optics design for the ANU linear booster accelerator"* **Nuclear Instruments and Methods in Physics Research Section A: Accelerators, Spectrometers, Detectors and Associated Equipment *382***: 172–175.

[5] G. Herbert, P. Charles, and L. S. John. *Classical Mechanics, 3rd ed*. India: Dorling Kindersley, 2005. Chap. 1.

[6] Z. Dimitrovová and T. Mazilu, (2024) *"Semi-Analytical Approach and Green's Function Method: A Comparison in the Analysis of the Interaction of a Moving Mass on an Infinite Beam on a Three-Layer Viscoelastic Foundation at the Stability Limit–The Effect of Damping of Foundation Materials"* **Materials *17***: 279. DOI: 10.3390/ma17020279.

[7] B. Nikolic, C. L. Carilli, and L. Torino, (2024) *"Two-dimensional synchrotron beam characterization from a single interferogram"* **Physical Review Accelerators and Beams *27***(11): 112802. DOI: 10 . 1103 / PhysRevAccelBeams.27.112802.

[8] H. Jia, T. Li, T. Wang, Y. Zhao, X. Zhang, H. Xu, Z. Liu, J. Liu, L. Lin, H. Xie, L. Feng, F. Wang, F. Zhu, J. Hao, S. Quan, K. Liu, and S. Huang, (2024) *"High-brightness megahertz-rate beam from a direct-current and superconducting radio-frequency combined photocathode gun"* **Physical Review Research *6***: 043165. DOI: 10.1103/PhysRevResearch.6.043165.

[9] Y. Le Guennec and E. Savin, (2011) *"A transport model and numerical simulation of the high-frequency dynamics of three-dimensional beam trusses"* **Journal of the Acoustical Society of America *130***(6): 3706. DOI: 10.1121/1.3651819.

[10] K. L. Brown, F. Rothacker, D. C. Carey, and F. National. *Beam TRANSPORT Systems*. Tech. rep. Report

issued as CERN-80-04 and NAL-Q1. CERN and NAL, 1983.

[11] S. Bernal. *A Practical Introduction to Beam Physics and Particle Accelerators, 3rd ed.* IOP Publishing, 2022.

[12] R. Roussel, (2021) *"Multiobjective Bayesian optimization for online accelerator tuning"* **Physical Review Accelerators and Beams *24***(6): 062801. DOI: 10.1103/PhysRevAccelBeams.24.062801.

[13] A. G. Shkvarunets and R. B. Fiorito, (2008) *"Vector electromagnetic theory of transition and diffraction radiation with application to the measurement of longitudinal bunch size"* **Physical Review Special Topics - Accelerators and Beams *11***: 012801. DOI: 10.1103/PhysRevSTAB.11.012801.

[14] M. Mansuripur, (2021) *"Gaussian beam optics"* **Optics and Photonics News *12***(1): 44–45.

[15] R. Singh, (2022) *"Longitudinal charge distribution measurement of nonrelativistic ion beams using coherent transition radiation"* **Physical Review Accelerators and Beams *25***(3): 032801. DOI: 10.1103/PhysRevAccelBeams.25.032801.

[16] S. A. Khan and R. Jagannathan, (2024) *"New matrix representation of the Maxwell equations based on the Riemann-Silberstein-Weber vector for a linear inhomogeneous medium"* **Results in Optics *17***: 100747. DOI: 10.1016/j.rio.2024.100747.

[17] S. M. Barnett, M. Babiker, M. J. Padgett, and S. M. Barnett, (2017) *"Optical orbital angular momentum Subject Areas"* **Philosophical Transactions of the Royal Society A *375***: 20150444. DOI: 10.1103/PhysRevA.45.8185.

[18] W. K. Kahn. *Mathematical methods of physics*. Brooklyn, N.Y, 2016. Chap. 5.

[19] Z. Slawomir and D. Leszek, (2014) *"Mathematical Model of the Damped Variable Cross Section Beam in Transportation"* **Advanced Materials Research *837***: 517–522. DOI: 10.4028/www.scientific.net/AMR.837.517.

[20] G. Ha, J. G. Power, E. E. Wisniewski, W. Liu, and M. Conde, (2021) *"Single-shot measurement of transverse second moments using the projection method"* **Physical Review Accelerators and Beams *24***(1): 012802. DOI: 10.1103/PhysRevAccelBeams.24.012802.

[21] N. J. Sammut, L. Bottura, P. Bauer, G. Velev, T. Pieloni, and J. Micallef, (2007) *"Mathematical formulation to predict the harmonics of the superconducting Large Hadron Collider magnets. II. Dynamic field changes and scaling laws"* **Physical Review Special Topics - Accelerators and Beams *10***(8): 082802. DOI: 10.1103/PhysRevSTAB.10.082802.

[22] D. Golish. *Gaussian Beam Optics*. 2006.

[23] A. A. Fakhri, P. Kant, G. Singh, and A. D. Ghodke, (2015) *"An analytical study of double bend achromat lattice"* **Review of Scientific Instruments**: 033304:1–11. DOI: 10.1063/1.4914389.

[24] L. E. L. D. Oskolovich, D. M. A. B. Bykov, A. A. L. Albert, M. Ingazov, and E. V. A. B. Abezus, (2019) *"Optimal mass transportation and linear assignment problems in the design of freeform refractive optical elements generating far-field irradiance distributions"* **Optics Express *27***(9): 13083–13097. DOI: 10.1364/OE.27.013083.

[25] R. Hessami and S. Gessner, (2023) *"Compact source of positron beams with small thermal emittance"* **Physical Review Accelerators and Beams *26***(12): 123402. DOI: 10.1103/PhysRevAccelBeams.26.123402.

[26] D. L. Knies, K. S. Grabowski, and C. Cetina, (2007) *"Ion optic calculations and installation of a modified SIMS ion source"* **Nuclear Instruments and Methods in Physics Research B *259***(1): 118–122. DOI: 10.1016/j.nimb.2007.01.150.